



Understanding the Effect of Calcination Process on the Mesoporous MCM-41 Material Morphology

Rahmiye Zerrin Yarbay Şahin^{1,2*}  

¹Bilecik Şeyh Edebali University Department of Chemical Engineering, 11210 Bilecik, Turkey

²Bilecik Şeyh Edebali University Energy Technologies Application and Research Centre, 11210 Bilecik, Turkey

The pore structure, which is known to be affected by calcination, is one of the desired features for materials especially when considered to be catalysts. The improvement in the structure occurs after removing all template ions during the calcination process. This study attempts to evaluate the impact of the calcination process on properties of mesoporous MCM-41 (Mobile Composition of Matter 41) obtained via sol-gel method. Characterization of calcined and untreated samples was performed by N₂ adsorption-desorption, scanning electron microscopy (SEM) and Fourier transform infrared spectroscopy (FT-IR) analysis. The results showed that the calcination process displayed a significant impact on the MCM-41 materials. After calcination, the MCM-41 sample possessed higher surface area and smaller pore diameter, compared to the untreated one. Finally, the calcination acted as an effective pore modulating procedure, thus giving a significant impact on the morphology of the studies of MCM-41. Therefore, the calcination step in MCM-41 material preparation is explained in detail ensuring valuable characterization information to the literature.

Keywords: Calcination effect; MCM-41; Sol-gel method; Uncalcined MCM-41.

Submitted: June 08, 2021. **Accepted:** July 12, 2021.

Cite this: Yarbay Şahin RZ. Understanding the Effect of Calcination Process on the Mesoporous MCM-41 Material Morphology. JOTCSB. 2021;4(2):27-32.

***Corresponding Author. E-mail:** zerrin.yarbay@bilecik.edu.tr

INTRODUCTION

Since porous materials are popular due to the ability to network with atoms, ions, and molecules, ordered mesoporous materials have gained great attention in science since 1992 (1). Among these materials, MCM-41 (Mobile Composition of Matter 41) which has a hexagonal array of uniformly sized one-dimensional pore geometry (2). Owing to their advantages like large specific surface areas and well-defined pore structures, these materials are ideal for many areas such as adsorption, separation, energy, and drug delivery systems. Among the applications, the most popular use of porous materials is the one that can be defined as a catalytic material. Therefore, the entrance of the heteroatoms inside these materials to make them catalytically active could result to a diminution in

the quality of the pore structure that could add onto the synthesis and calcination parameters (3).

Crystalline products with varied compositions, structures, and morphologies could be attained by altering the calcination conditions such as temperature, duration, and heating rate (4). As calcination is known as an endothermic reaction, temperature in the calcination zone of the particle declines and a heat transfer which is significantly affected by particle size arises from the particle surroundings to the relevant zone (5).

Although many studies deal with MCM-41 synthesis in terms of factors such as different synthesis methods (6-8), calcination temperature (9), and calcination atmosphere (10,11). Martínez-Edo et al. published a comprehensive paper related to synthesis and applications of MCM-41 in catalysis.

They reviewed some catalytic systems using mono and di-functionalized MCM-41 as basic and acidic catalysts based on metallic complexes supported by MCM-41, metallic nanoparticles embed onto functionalized MCM-41 and magnetic MCM-41. They underlined that although the supports like SBA-15, MCM-41 are cheap, synthetically versatile, and can be reused, an advantage over other systems is that MCM-41 have been extensively studied due to their applications in biological applications. Furthermore, the chemical versatility of MCM-41 relies not only on the easy preparation of the molecular sieves, but also on the straightforward regioselective functionalization, both within the inner walls of the pores and the outside surface of the particle (12). Wu et al. studied graded synthesis of highly ordered MCM-41 and carbon/zeolite composite from coal gasification fine residue for crystal violet removal. They found that MCM-41 with large BET of 1013 m²/g exhibited five characteristics diffraction peaks. They stated that the common silicon sources like ethyl orthosilicate (TEOS) or sodium metasilicate are of high cost. Therefore, cheap solid waste as an alternative raw material has a significant advantage and also environmental protection. They used filtrate from the lower layer in alkaline condition from coal gasification fine residue was used as silicon sources to further synthesize MCM-41. They found that the remove ratio of crystal violet in water by the synthesized MCM-41 is higher than 99% with a concentration in the range of 50-400 mg/L (13). Manaa et al. investigated MCM-41 grafted with citric acid. MCM-41 was synthesized via a sol-gel method and then grafted by adding the appropriate amount of citric acid (CA). The pore sizes and volume of the CA/MCM-41 samples were found to vary markedly within CA contents. The catalytic performance of the samples was tested by the synthesis of 14-Phenyl-14H-dibenzo [a, j] xanthene (xanthene). In this reaction, the sample with 50 wt.% of CA displayed the highest acidity and catalytic activity (14). Gedikli et al. synthesized MCM-41 via hydrothermal and sonochemical synthesis methods. Their results showed that MCM-41 synthesized by the sonochemical method had higher specific surface area and pore volume than those synthesized by the hydrothermal method. Also, they investigated the effects of silica sources on the distribution of products. They found that the sodium silicate was found to be more suitable for the synthesis of MCM-41. Based on their determined optimum conditions, they also studied synthesis and characterization of MCM-41 supported Al, Co, and Fe having different ratios of metal (Metal/Si: ratio 0.05, 0.1, and 0.2). As a result, they offered to explore the catalytic properties of these catalysts (15). Laghei et al. investigated the effect of various types of post-synthetic modifications on the structure and

properties of MCM-41 mesoporous silica. They synthesized MCM-41 mesoporous silicas by hydrothermal method were subsequently modified by 3-aminopropyltrimetoxysilane (APTMS) and trimethylchlorosilane (TMCS) via two different grafting methods, i.e. attaching functional groups with or without solvent. The results confirmed that the spherical MCM-41 particles were successfully functionalized by APTMS and TMCS. Moreover, the surface area and average pore diameters of the particles were affected by the inherent properties of organosilanes such as their side chains and catalytic behaviors. The grafting methods had a tremendous impact on the obtained treated particles (16).

Among many studies, only a few studies (8) explored the differences between untreated and calcined MCM-41 samples. Therefore, this study will contribute to the literature with the help of providing more details about the calcination effect on MCM-41. In this study, MCM-41 materials were obtained via adapted sol-gel method and characterized by N₂ adsorption-desorption, Fourier transformed infrared spectroscopy (FT-IR) and scanning electron microscopy (SEM). The influence of the calcination process on the properties are discussed in detail in the discussion section.

MATERIAL AND METHOD

Sample Preparation

MCM-41 material was attained by a modified sol-gel procedure given by Martin et al. (12). Analytical grade reagents including Cetyltrimethylammonium bromide (CTAB-Alfa Aesar, 98%) by means of structure directing agent, tetraethyl orthosilicate (TEOS-Acros, 98%) by way of silica source were utilized as received. In addition, absolute ethanol (Tekkim, >99.5%), hydrochloric acid (VWR, 37%), and ammonia (Carlo Erba, 25%) were the other reagents used. According to the procedure, 40 mL of distilled water, 6 mL of ammonia, 2 g of CTAB, 60 mL of ethanol and 4 mL of TEOS were mixed using strong magnetic stirring at 30 °C for 2 h. Afterwards, a white precipitate was obtained by filtration and washed thoroughly with distilled water (12). The material obtained was divided into two parts. While half of the sample was not subjected to calcination procedure (labelled as untreated sample), the other half was calcined at 550 °C for during 6 hours in air atmosphere in a muffle furnace with 5 °C/min to eliminate the CTAB from the sample.

Characterization

The textural properties of the MCM-41s were obtained from N₂ adsorption/desorption isotherms using Micromeritics ASAP 2020 equipment. While specific surface areas were considered with respect to the Brunauer-Emmett-Teller (BET) method, the

pore size distributions were achieved using the Barret–Joyner–Hallenda (BJH) method from the N₂ adsorption/desorption isotherms. The structure was examined by SEM analysis on a Zeiss Supra VP 40 using SE2 detector at 15 kV. FT-IR spectra were logged using the Cary 630 FTIR spectrometer using the ATR technique (with a diamond-protected Attenuated Total Reflectance crystal unit) with a resolution of 4 cm⁻¹ after 100 scans in the 4000–500 cm⁻¹ wavelength range.

RESULTS AND DISCUSSION

The effect of calcination process on MCM-41 mesoporous materials are investigated in this study. Therefore, the characteristics of calcined and untreated MCM-41 were examined in detail in this section.

The surface area analysis is given in Table 1. The surface area of the untreated MCM-41 was

measured as 548.17 m²/g which is very low in proportion to the calcined one (1245.24 m²/g). This situation can be explained as the mesopores occupied by the surfactant molecules thus dropping the specific surface area. While the total pore volume of untreated MCM-41 was measured as 0.18 cm³/g, the total pore volume of calcined MCM-41 was 0.48 cm³/g. The pore diameter values of the both samples were quite similar.

The surface area of the untreated MCM-41 was quite improved when compare to the other studies in the literature (15, 18-20). Due to high surface, calcined MCM-41 material can be evaluated as promising catalyst candidate for the various applications like photocatalytic applications, adsorption, pyrolysis of the biomass, etc. Therefore, the catalytic properties of the material are worth to investigate.

Table 1: Surface area analysis of the MCM-41s.

MCM-41	Surface area (m ² /g)	Pore volume (cm ³ /g)	Average pore diameter (Å)
Untreated	548.17	0.18	18.15
Calcined	1245.2	0.48	19.00

The N₂ adsorption/desorption isotherms of the materials are given in Figure 1. Both MCM-41 samples showed similar tendencies. Depending on the IUPAC classification, type IV classification is appropriate for the mesoporous nature of the materials and reliable with previous studies. Besides, a H1-type hysteresis loop which was the appearance of mesoporous silicas was observed.

The adsorption/desorption isotherms altered slowly at a lower P/P⁰ stage, where nitrogen molecules shielded the mesoporous walls with monolayer adsorption. Besides, these isotherms showed a sharp inflection at P/P⁰ = 0.15–0.35, which confirmed that capillary condensation arose in uniform mesopores. This can be related to the N₂ molecules shielded the mesoporous walls with monolayer and multilayer adsorption. As a result,

adsorption/desorption isotherms results pointed out the presence of mesoporous structure (21).

The calcination process is known to affect the morphologies of the materials. Figure 2 displays SEM micrographs of the MCM-41s before and after the calcination process. There is no significant difference in MCM-41 framework with spherical particles with similar particle diameters. It is noticeable that most particles were almost perfectly spherical although some agglomerates were visible after calcination. This tendency could be associated with the fact that the interaction of minor particles resulted in their aggregation into numerous spherical particles with greater sizes. Besides, a huge amount of mesopores formed after the aggregation of primary units or crystallites (4).

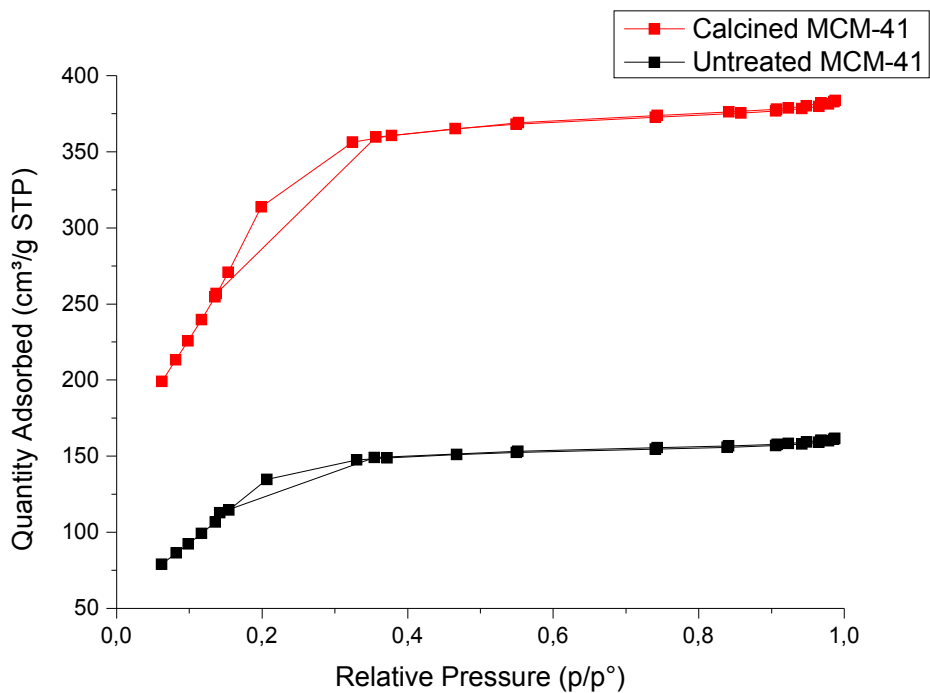


Figure 1: Nitrogen isotherms of the MCM-41s.

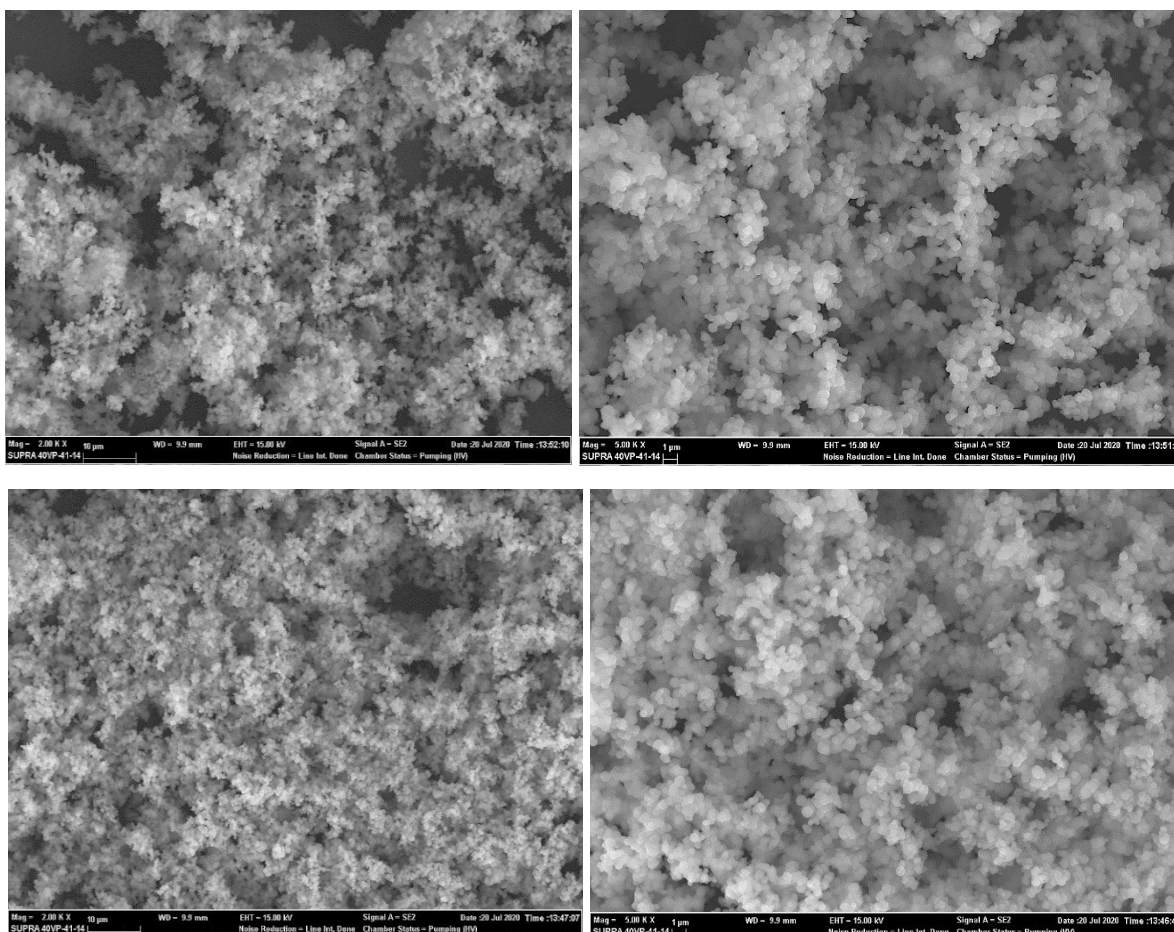


Figure 2: SEM micrographs of untreated MCM-41 (a) 2000 zoom, (b) 5000 zoom, and calcined MCM-41 (c) 2000 zoom, (d) 5000 zoom.

The FT-IR spectra are utilized to control the frequency variation in the functionality on the surfaces. FT-IR results of the MCM-41s is shown in Figure 3. It is believed that the existence of absorption bands around 2927 and 2852 cm^{-1} for the untreated sample corresponded to asymmetric and symmetric CH_2 vibrations of the organic surfactant molecules (22). The peak at 1650 cm^{-1} responded to the surface-adsorbed hydroxyl groups (4). According to Wang et al., the existence of the hydroxyl groups on the surface serves to improve of catalytic activity in such applications like photocatalytic systems due to their interacting ability with photogenerated holes to result in improved charge transfer and prevent the recombination of electron-hole pairs (4). The characteristic band for ammonium ions could be realized at 1405.57-1529.90 cm^{-1} (23). FT-IR spectra of the both materials showed the typical characteristic peaks of silica at ~ 1045 -790 cm^{-1} , agreeing to the vibrations of the Si-O-Si symmetric bond, Si-OH stretching bond and Si-O-Si asymmetric bond (23, 24). The O-H out of plane bending peak was detected at 564 cm^{-1} for only untreated MCM-41 (25).

Any band at 3500 cm^{-1} related to O-H stretching of surface hydroxyl groups indicating hydroxyl groups

and water molecules adsorbed was not detected. Besides, surface-adsorbed hydroxyl groups decreased indistinctly after calcination. In the calcined MCM-41 spectrum, the absorption peaks of 2924 cm^{-1} , 2848 cm^{-1} , and 1477 cm^{-1} existing in the untreated MCM-41 sample were vanished, signifying that CTAB was eliminated (24).

CONCLUSION

The objective of this study was to evaluate the calcination process influence on the structural properties of MCM-41. Therefore, the study dealt with the characteristic differences between untreated and calcined MCM-41 samples in terms of N_2 adsorption-desorption, FT-IR, and SEM techniques. The results demonstrate that the calcination process displays a noticeable impact on the structures. The surface area was especially improved with the calcination process. It is especially significant to highlight that some of the absorption peaks that existed in the untreated MCM-41 sample disappeared after calcination, thus signifying that the surfactants were eliminated. Further studies of the modification of the MCM-41 prepared according to this study with different metal species and catalytic applications of these materials are underway.

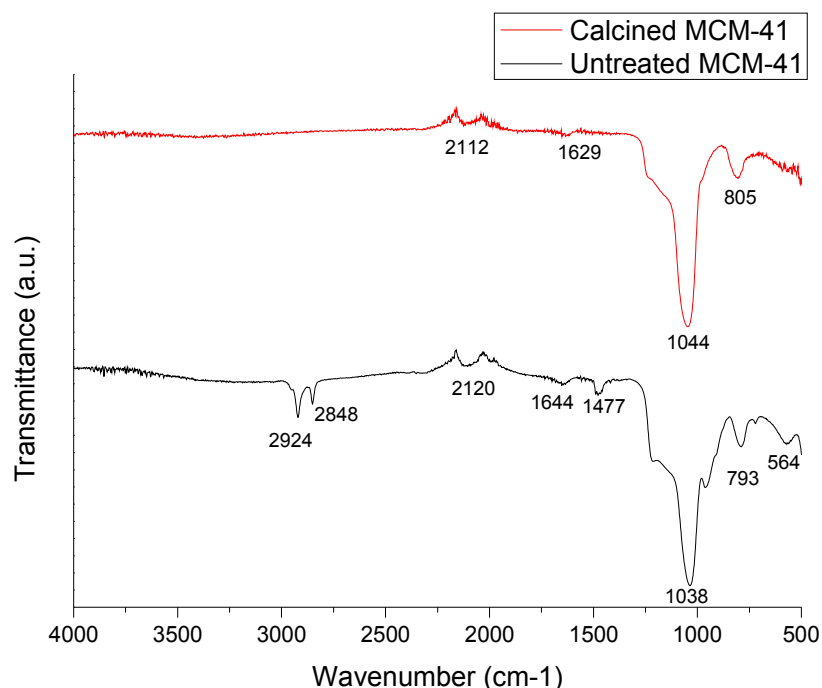


Figure 3: FT-IR spectra of the MCM-41s.

FUNDING

This study did not receive any specific grant from funding agencies in the public, commercial, or not-for-profit sectors.

REFERENCES

1. Logar N, Kaučič V. Nanoporous materials: From catalysis and hydrogen storage to wastewater treatment. *Acta Chim Slov.* 2006;53(2):117–35.

2. Dhal JP, Dash T, Hota G. Iron oxide impregnated mesoporous MCM-41: synthesis, characterization and adsorption studies. *J Porous Mater.* 2020;27(1):205–16. DOI: <https://doi.org/10.1007/s10934-019-00803-0>.
3. Galacho C, Carrott M, Carrott P. Effect of calcination parameters on structural properties of Ti-MCM-41 materials synthesized at room temperature. In: *Actas do XX Encontro Nacional da Sociedade Portuguesa de Química Campus da Caparica* [Internet]. 2006. p. 209. Available from: <https://dspace.uevora.pt/rdpc/handle/10174/6338>.
4. Wang G, Xu L, Zhang J, Yin T, Han D. Enhanced Photocatalytic Activity of Powders (P25) via Calcination Treatment. *International Journal of Photoenergy.* 2012;2012:1–9. DOI: <https://doi.org/10.1155/2012/265760>.
5. García-Labiano F, Abad A, de Diego LF, Gayán P, Adánez J. Calcination of calcium-based sorbents at pressure in a broad range of CO₂ concentrations. *Chemical Engineering Science.* 2002;57(13):2381–93. DOI: [https://doi.org/10.1016/S0009-2509\(02\)00137-9](https://doi.org/10.1016/S0009-2509(02)00137-9).
6. Lourenço JP, Fernandes A, Henriques C, Ribeiro MF. Al-containing MCM-41 type materials prepared by different synthesis methods: Hydrothermal stability and catalytic properties. *Microporous and Mesoporous Materials.* 2006;94(1–3):56–65. DOI: <https://doi.org/10.1016/j.micromeso.2006.03.020>.
7. Sohrabnezhad Sh, Jafarzadeh A, Pourahmad A. Synthesis and characterization of MCM-41 ropes. *Materials Letters.* 2018;212:16–9. DOI: <https://doi.org/10.1016/j.matlet.2017.10.059>.
8. Laghaei M, Sadeghi M, Ghalei B, Dinari M. The effect of various types of post-synthetic modifications on the structure and properties of MCM-41 mesoporous silica. *Progress in Organic Coatings.* 2016;90:163–70. DOI: <https://doi.org/10.1016/j.porgcoat.2015.10.007>.
9. He N, Lu Z, Yuan C, Hong J, Yang C, Bao S, et al. Effect of trivalent elements on the thermal and hydrothermal stability of MCM-41 mesoporous molecular materials. *Supramolecular Science.* 1998;5(5–6):553–8. DOI: [https://doi.org/10.1016/S0968-5677\(98\)00073-X](https://doi.org/10.1016/S0968-5677(98)00073-X).
10. Fellenz NA, Bengoa JF, Marchetti SG, Gervasini A. Influence of the Brønsted and Lewis acid sites on the catalytic activity and selectivity of Fe/MCM-41 system. *Applied Catalysis A: General.* 2012;435–436:187–96. DOI: <https://doi.org/10.1016/j.apcata.2012.06.003>.
11. Yin A, Wen C, Dai W-L, Fan K. Ag/MCM-41 as a highly efficient mesostructured catalyst for the chemoselective synthesis of methyl glycolate and ethylene glycol. *Applied Catalysis B: Environmental.* 2011;108–109:90–9. DOI: <https://doi.org/10.1016/j.apcatb.2011.08.013>.
12. Martin P, Rafti M, Marchetti S, Fellenz N. MCM-41-based composite with enhanced stability for Cr(VI) removal from aqueous media. *Solid State Sciences.* 2020;106:106300. DOI: <https://doi.org/10.1016/j.solidstatesciences.2020.106300>.
13. Chen H, Fu S, Fu L, Yang H, Chen D. Simple Synthesis and Characterization of Hexagonal and Ordered Al-MCM-41 from Natural Perlite. *Minerals.* 2019;30;9(5):264. DOI: <https://doi.org/10.3390/min9050264>.
14. Boukoussa B, Hamacha R, Morsli A, Bengueddach A. Adsorption of yellow dye on calcined or uncalcined Al-MCM-41 mesoporous materials. *Arabian Journal of Chemistry.* 2017;10:S2160–9. DOI: <https://doi.org/10.1016/j.arabjc.2013.07.049>.
15. Mangrulkar PA, Kamble SP, Meshram J, Rayalu SS. Adsorption of phenol and o-chlorophenol by mesoporous MCM-41. *Journal of Hazardous Materials.* 2008;160(2–3):414–21. DOI: <https://doi.org/10.1016/j.jhazmat.2008.03.013>.
16. Lu D, Xu S, Qiu W, Sun Y, Liu X, Yang J, et al. Adsorption and desorption behaviors of antibiotic ciprofloxacin on functionalized spherical MCM-41 for water treatment. *Journal of Cleaner Production.* 2020;264:121644. DOI: <https://doi.org/10.1016/j.jclepro.2020.121644>.
17. Kunchakara S, Ratan A, Dutt M, Shah J, Kotnala RK, Singh V. Impedimetric humidity sensing studies of Ag doped MCM-41 mesoporous silica coated on silver sputtered interdigitated electrodes. *Journal of Physics and Chemistry of Solids.* 2020;145:109531. DOI: <https://doi.org/10.1016/j.jpcs.2020.109531>.
18. Martínez-Edo G, Balmori A, Pontón I, Martí del Río A, Sánchez-García D. Functionalized Ordered Mesoporous Silicas (MCM-41): Synthesis and Applications in Catalysis. *Catalysts.* 2018;8(12):617. DOI: <https://doi.org/10.3390/catal8120617>.
19. Wu Y-H, Ma Y-L, Sun Y, Xue K, Ma Q-L, Ma T, et al. Graded synthesis of highly ordered MCM-41 and carbon/zeolite composite from coal gasification fine residue for crystal violet removal. *Journal of Cleaner Production.* 2020;277:123186. DOI: <https://doi.org/10.1016/j.jclepro.2020.123186>.

20. A. Mannaa M, Altass HM, Salama RS. MCM-41 grafted with citric acid: The role of carboxylic groups in enhancing the synthesis of xanthenes and removal of heavy metal ions. *Environmental Nanotechnology, Monitoring & Management*. 2021;15:100410. DOI: <https://doi.org/10.1016/j.enmm.2020.100410>.
21. Gedikli Ü, Mısırlıoğlu Z, Acar Bozkurt P, Canel AM. SYNTHESIS AND CHARACTERIZATION OF MCM-41 AND METAL-SUPPORTED MCM-41 MATERIALS USING DIFFERENT METHODS. *Commun Fac Sci Univ Ankara Ser B: Chem Chem Eng*. 2020;62(2):23–39.
22. Laghaei M, Sadeghi M, Ghalei B, Dinari M. The effect of various types of post-synthetic modifications on the structure and properties of MCM-41 mesoporous silica. *Progress in Organic Coatings*. 2016;90:163–70. DOI: <https://doi.org/10.1016/j.porgcoat.2015.10.007>.
23. Hui KS, Chao CYH. Synthesis of MCM-41 from coal fly ash by a green approach: Influence of synthesis pH. *Journal of Hazardous Materials*. 2006;137(2):1135–48. DOI: <https://doi.org/10.1016/j.jhazmat.2006.03.050>.
24. Lensveld DJ, Gerbrand Mesu J, Jos van Dillen A, de Jong KP. Synthesis and characterisation of MCM-41 supported nickel oxide catalysts. *Microporous and Mesoporous Materials*. 2001;44–45:401–7. DOI: [https://doi.org/10.1016/S1387-1811\(01\)00214-1](https://doi.org/10.1016/S1387-1811(01)00214-1).
25. Li Q, Brown SE, Broadbelt LJ, Zheng J-G, Wu NQ. Synthesis and characterization of MCM-41-supported Ba₂SiO₄ base catalyst. *Microporous and Mesoporous Materials*. 2003;59(2–3):105–11. DOI: [https://doi.org/10.1016/S1387-1811\(03\)00290-7](https://doi.org/10.1016/S1387-1811(03)00290-7).

